Development of a tunable method for PID controllers to achieve the desired phase margin

Sergei S. Mikhalevich [a,*], Sergey A. Baydali [a], Flavio Manenti [b]

[a] *National Research Tomsk Polytechnic University, Institute of Physics and Technology, Department of Electronics and Automation of Nuclear Plants, Tomsk 634050, Russia*

[b] *Politecnico di Milano, Dept. di Chimica, Materiali e Ingegneria Chimica "Giulio Natta", Piazza Leonardo da Vinci 32, 20133 Milano, Italy*

Received 27 March 2014
Received in revised form 29 October 2014
Accepted 29 October 2014

1. Introduction

The proportional-integral-derivative (PID) controllers are widely used in industry [1]. They are applied for solving a wide range of tasks, mainly regulatory and servomechanism problems in process industry, aviation, and power generation plants to quote a few. Moreover, also DVD players and HDD-disks implement PID controllers, and their use is in the form of a separate device or as a software-based algorithm.

Several methods for the selection of the optimal adjustment parameters of PI/PID controllers have been developed since the 60ies of the previous century and nowadays a huge number of them are available [1–5]. The most of them select the controller adjustment parameters according to the provision conditions of the required system quality index. Controllers can be adjusted by various criteria such as by time (setting time and overshoot), frequency (phase and amplitude stability margin, preset upper bound of a sensitivity function), integrals, etc. The frequency methods for the regulators tuning are nowadays widely used since they allow to evaluate the stability and the performances of a control system in a direct or indirect manner. Nevertheless, all the methods present pros and cons; the Ziegler–Nichols method, for instance, despite its popularity because of its simplicity of application, provides high overshoot and large setting time [6].

A method for determining the controller setting parameters based on setting the stability margin is broached in this paper. The phase margin stability indirectly characterizes the system stability in the frequency domain. It is recommended as a criterion for the control systems setting [7], and is a necessary but not sufficient condition for system stability [8].

2. Assumptions

The phase and amplitude margins are known to be indirect features of the system stability in the frequency domain. As reported in the scientific literature, the system phase stability margin should be in the range of 30–60 degrees [7,9]. Such parameters are widely used as criteria for the synthesis of automatic control systems and for the calculation of controller settings [6,7].

The typical control system of Fig. 1 with equal phase margin stability but different types of Nyquist curves is selected to assess different controller settings available from several experiments (Table 1). The analysis is reported in Fig. 2 and it illustrates that a positive overshoot is absent or minimal when the curve is vertically raised up until it intersects with the unit circle with the center in the origin. When the crossover frequency increases, the deviation of the curve from the ordinate is observed and the nonlinear change of overshooting is noted as well.

* Corresponding author. Tel.: +7 3822427096.
E-mail addresses: AnopT@ya.ru, mihalevichss@tpu.ru (S.S. Mikhalevich).

Table 1
Parameters of the observed control system.

Plant model	Phase margin, deg	Crossover frequency, rad/s	k_p	k_i	k_d
$\frac{s-1}{(2s+1)^3}e^{-0.5s}$	60	0.05	0.1511	−0.0465	1.4639
	60	0.2	−0.9712	−0.1935	−1.1034
	60	0.3	−1.5184	−0.3068	−3.2481

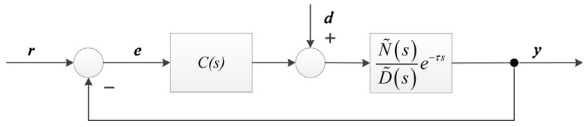

Fig. 1. Block diagram of a process with a PID controller.

Consequently, the following condition must be fulfilled to minimize the overshoot:

$$\frac{dRe[G(j\omega)]}{d\omega} = 0, \tag{1}$$

where $G(j\omega)$ is the transfer function of the open-loop system.

The qualitative scheme of the selected system is presented in Fig. 1 and the typical Nyquist curve of such a system is reported in Fig. 3.

It is mandatory that the modulus of the open-loop transfer function have not any resonance peak [9] to prevent any overshooting in the step response (Fig. 4). Such a principle has been adopted in the modulus optimum criteria [7].

The modulus of the open-loop transfer function on the Bode plot is presented in the following form:

$$\frac{A(\omega)}{A(0)} = \frac{|G(j\omega)|}{|G(0)|} = \frac{\sqrt{R^2(\omega)+I^2(\omega)}}{\sqrt{R^2(0)+I^2(0)}} = \frac{\sqrt{R^2(\omega)+I^2(\omega)}}{c}, \tag{2}$$

where $R(\omega)$ and $I(\omega)$ are the real and imaginary part of the open-loop system, respectively, and c is a constant. Then, the real part of $G(j\omega)$ is stated as follows:

$$\left(\frac{A(\omega)}{A(0)}\right)^2 = \frac{|G(j\omega)|^2}{|G(0)|^2} = \frac{R^2(\omega)+I^2(\omega)}{c^2} = 1, \tag{3}$$

$$R(\omega) = \pm\sqrt{c^2 - I^2(\omega)}, \tag{4}$$

$$\frac{dR(\omega)}{d\omega} = \pm\frac{d\sqrt{c^2 - I^2(\omega)}}{d\omega}, \tag{5}$$

According to the condition (5), the derivative of the real part of $G(j\omega)$ has two solutions.

As it is possible to note from Fig. 3, the imaginary part of $G(j\omega)$ reduces, when the frequency is less than the crossover frequency.

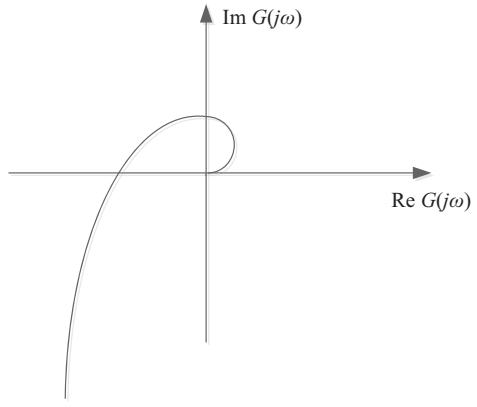

Fig. 3. Typical view of the Nyquist curve.

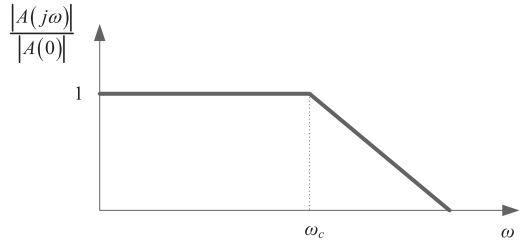

Fig. 4. Magnitude of the open-loop transfer function.

This means that the square of the function $I^2(\omega)$ is reduced too. According to Fig. 4, in order to avoid any overshoot in the step response, the following condition has to be fulfilled:

$$-\frac{d\sqrt{c^2 - I^2(\omega)}}{d\omega} \le \frac{dR(\omega)}{d\omega} \le \frac{d\sqrt{c^2 - I^2(\omega)}}{d\omega}. \tag{6}$$

The point is to obtain one solution only from Eq. (5) and, next, to express the control parameters as a function of this solution; to do so, we may search for a particular solution, which is the one when the derivative of the real part of $G(j\omega)$ is null. As a result, we obtain the condition (1).

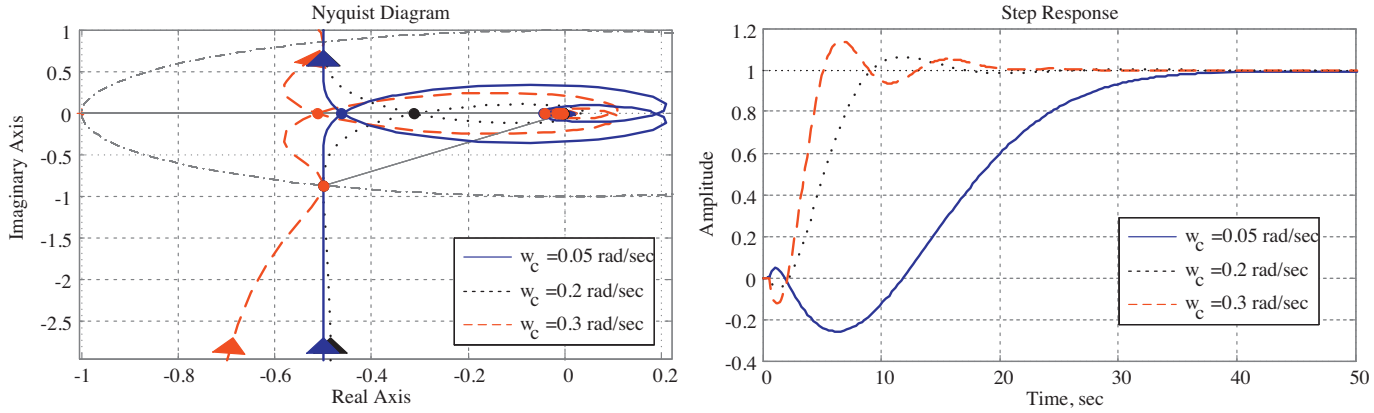

Fig. 2. The Nyquist curve influence on the behavior of the time response.

Hence, condition (1) provides the vertical rise of the Nyquist curve until it intersects the unitary circle with the center in the origin.

3. Mathematical description of the method

The qualitative scheme of the selected control system is presented in Fig. 1. The system consists of a controller $C(s)$ and controlled system (e.g., industrial unit) with the lagging, included in a negative feedback loop. The preset value is pointed out by r, the system output by y, and the load disturbances by d.

To avoid further transcendent equations, lagging should be expanded into the series of Padé and proposed in the following form:

$$e^{-\tau s} = \frac{L(s)}{M(s)}. \tag{7}$$

As a result, the controlled system is written in general terms as follows:

$$P = \frac{\widetilde{N}(s)}{\widetilde{D}(s)} \cdot e^{-\tau s} = \frac{\widetilde{N}(s)}{\widetilde{D}(s)} \cdot \frac{L(s)}{M(s)} = \frac{N(s)}{D(s)}. \tag{8}$$

The controller assumes the following form:

$$C = \left(K_1 + \frac{K_2}{s} + K_3 \cdot s\right). \tag{9}$$

By inserting $s = j\omega$, the controlled system and the controller are stated, respectively, as follows:

$$P(s) = \frac{N(s)}{D(s)} = \frac{N_e(\omega) + j\omega N_o(\omega)}{D_e(\omega) + j\omega D_o(\omega)}, \tag{10}$$

$$C(j\omega) = \left(K_1 + \frac{K_2}{j\omega} + K_3 \cdot j\omega\right). \tag{11}$$

For the sake of conciseness of the mathematical formulation, we will omit $(j\omega)$ thereafter. The transfer function of the open-loop $G(j\omega) = C(j\omega)P(j\omega)$ is:

$$G = \frac{\omega^2 N_o K_1 - K_2 N_e + \omega^2 K_3 N_e}{\omega^2 D_o - j\omega D_e} - j\frac{(\omega K_1 N_e + \omega N_o K_2 - \omega^3 K_3 N_o)}{\omega^2 D_o - j\omega D_e}. \tag{12}$$

According to the determination of the absolute stability margin by means of the Nyquist curve [7], we can formulate the system of equations that guarantees the presence of the preset phase stability margin, φ_m, and the fulfillment of the condition (1) as well:

$$\begin{aligned} &ReG(j\omega_c) = -\cos(\varphi_m), \\ &ImG(j\omega_c) = -\sin(\varphi_m), \\ &\frac{dRe\,[G(j\omega_c)]}{d\omega_c} = 0, \end{aligned} \tag{13}$$

where φ_m is the phase margin.

Substituting Eq. (12) into the system above (13), we obtain an algebraic equations system for the calculation of the desired parameters of the PID-controller:

$$\begin{aligned} &K_1 a_{11} + K_2 a_{12} + K_3 a_{13} = b_1, \\ &K_1 a_{21} + K_2 a_{22} + K_3 a_{23} = b_2, \\ &K_1 a_{31} + K_2 a_{32} + K_3 a_{33} = 0 \end{aligned} \tag{14}$$

with the equation coefficients stated as follows:

$$\begin{aligned} a_{11} &= \omega^4 N_o D_o + \omega^2 N_e D_e, \\ a_{12} &= \omega^2 N_o D_e + \omega^2 N_e D_o, \\ a_{13} &= \omega^4 N_e D_o + \omega^4 N_o D_e, \end{aligned} \tag{15}$$

$$\begin{aligned} a_{21} &= \omega^3 N_o D_e + \omega^3 N_e D_o, \\ a_{22} &= -\omega N_e D_e + \omega^3 N_o D_o, \\ a_{23} &= \omega^3 N_e D_e + w^5 N_o D_o, \end{aligned} \tag{16}$$

$$\begin{aligned} a_{31} &= \omega^8(N'_o D_o^3 - N_o D'_o D_o^2) + \omega^6(N'_o D_e^2 D_o + N_o D_e^2 D'_o + N'_e D_e D_o^2 + N_e D'_e D_o^2 - 2N_o D'_e D_e D_o - 2N_e D_e D'_o D_o) + \omega^5(2N_o D_e^2 D_o - 2N_e D_e D_o^2) + \omega^4(N'_e {D_e}^3 - N_e D'_e D_e^2), \\ a_{32} &= \omega^6(N'_o D_e D_o^2 - N'_e D_o^3 + N_e D'_o D_o^2 + N_o D'_e D_o^2 - 2N_o D_e D'_o D_o) + \omega^5(2N_e D_o^3 - 2N_o D_e D_o^2) + \omega^4(N'_o D_e^3 - N'_e D_e^2 D_o - N_e D_e^2 D'_o + 2N_e D'_e D_e D_o - N_o D'_e D_e^2), \\ a_{33} &= \omega^8(N'_e D_o^3 - N_e D'_o D_o^2 - N'_o D_e D_o^2 - N_o D'_e D_o^2 + 2N_o D_e D'_o D_o) + \omega^6(N'_e D_e^2 D_o + N_e D_e^2 D'_o - N'_o D_e^3 + N_o D'_e {D_e}^2 - 2N_e D'_e D_e D_o) + \omega^5(2N_e D_e^2 D_o - 2N_o D_e^3), \end{aligned} \tag{17}$$

$$\begin{aligned} b_1 &= -\cos\varphi(\omega^2 {D_e}^2 + \omega^4 {D_o}^2), \\ b_2 &= -\sin\varphi(\omega^2 {D_e}^2 + \omega^4 {D_o}^2). \end{aligned} \tag{18}$$

The solution of the algebraic system leads to the expressions for K_1, K_2, K_3:

$$K_1(\omega_c) = \frac{a_{13}a_{32}b_2 + a_{22}a_{33}b_1 - a_{12}a_{33}b_2 - a_{23}a_{32}b_1}{\Delta}, \tag{19}$$

$$K_2(\omega_c) = \frac{a_{11}a_{33}b_2 - a_{13}a_{31}b_2 - a_{21}a_{33}b_1 + a_{23}a_{31}b_1}{\Delta}, \tag{20}$$

$$K_3(\omega_c) = \frac{a_{12}a_{31}b_2 - a_{11}a_{32}b_2 + a_{21}a_{32}b_1 - a_{22}a_{31}b_1}{\Delta}, \tag{21}$$

with $\Delta = a_{11}a_{22}a_{33} - a_{11}a_{23}a_{32} - a_{12}a_{21}a_{33} + a_{12}a_{23}a_{31} + a_{13}a_{21}a_{32} - a_{13}a_{22}a_{31}$.

As it can be seen from the formulae (19)–(21), it is necessary to set the crossover frequency to calculate the PID controller tuning parameters. It is known that when the crossover frequency increases, the transient process time decreases, but the oscillations in the system increase [7].

To select the crossover frequency, the suggestion is to adopt the integral of time-weighted absolute error (ITAE):

$$\text{ITAE} = \int_0^\infty t\left|e(t)\right| dt, \tag{22}$$

where t is the time; and $e(t)$ is the converted deviation [10].

4. Examples

Let us consider the following controlled system of the third order with pure time delay (Example 1):

$$P(s) = \frac{1}{(s+1)(s^2+s+5)} e^{-2s}. \tag{23}$$

The crossover frequency $\varphi_m = 60^\circ$ for the system is adopted and the parameters are calculated by means of the formulae (19)–(21). The transient behavior of the system related to the crossover frequency as a tuning parameter is reported in Fig. 5. The Nyquist curves are presented in Fig. 6.

The advantage of the proposed method is in the possibility to select the crossover frequency, which allows to determine the transfer characteristic form. In accordance with the technological requirements of the industry and industrial processes, the controller can be set for:

- low frequency as to provide the transient process with the least overshoot;
- and for high frequency as to achieve a significant acceleration of the process dynamics (in this case some overshoot is present).

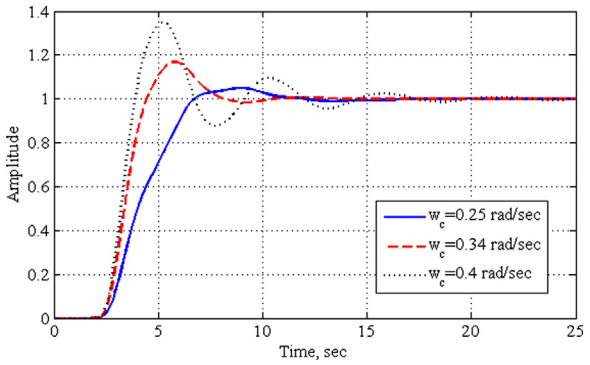

Fig. 5. Transient responses in the system depending on the crossover frequency.

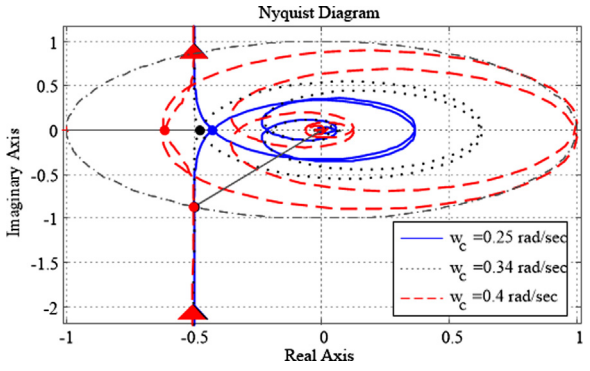

Fig. 6. The Nyquist curves of the control systems with different crossover frequency.

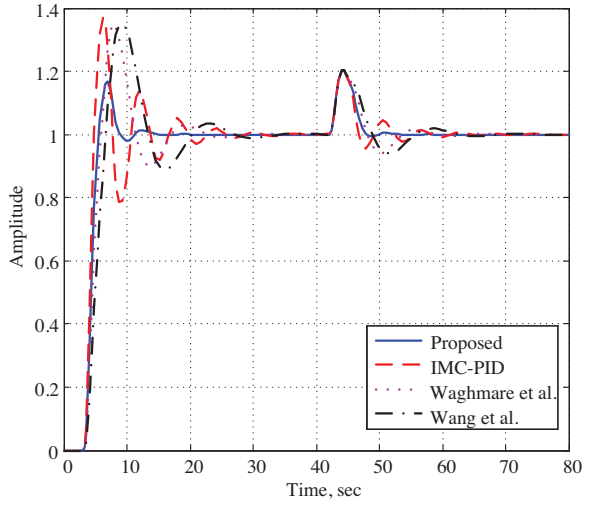

Fig. 7. The time responses comparison of the control systems in example 1 that were tuned by the proposed method and several known methods.

Using the integral of time-weighted absolute error (ITAE), the optimum crossover frequency is chosen and the controller adjustment parameters are achieved:

$$C(s) = 2.6921 + \frac{1.6226}{s} + 1.1409s. \tag{24}$$

To assess the effectiveness of the proposed method in estimating the PID-controller tuning parameters, it is necessary to compare it with the existing methods (desired phase margin is 60°). The

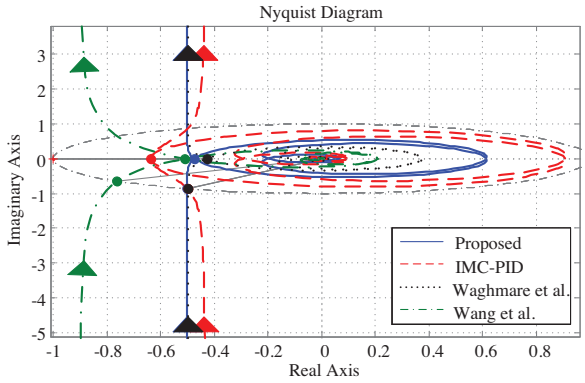

Fig. 8. The Nyquist curves comparison of the control system in example 1 with different PID controller parameters.

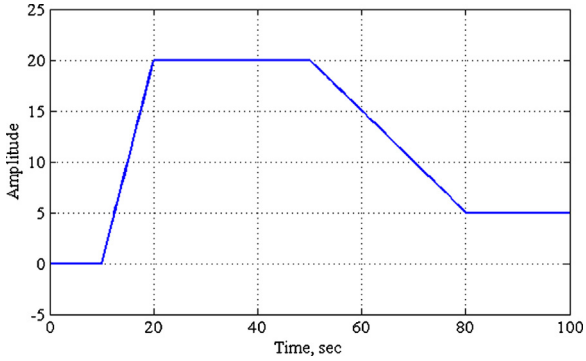

Fig. 9. The ramp disturbance case.

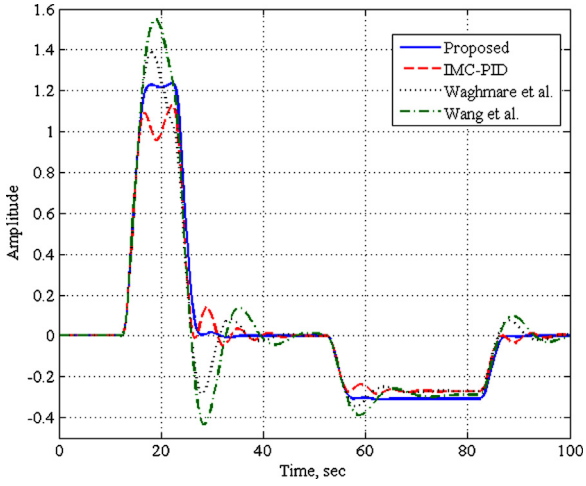

Fig. 10. Influence of the ramp disturbance to the transient responses in example 1.

methods proposed by IMC-PID [11,12], Waghmare et al. [13], Wang et al. [14] lead to the following controllers, respectively:

$$\begin{aligned} C_{\text{IMC-PID}}(s) &= 3.7298 + \frac{1.8432}{s} + 1.7709s, \\ C_{\text{Waghmare}}(s) &= 1.843 + \frac{1.35}{s} + 0.1686s, \\ C_{\text{Wang}}(s) &= 0.9901 + \frac{1.723}{s} + 0.2726s. \end{aligned} \tag{25}$$

The transient responses of the control system tuned by means of different methods are shown in Fig. 7. The Nyquist curves are

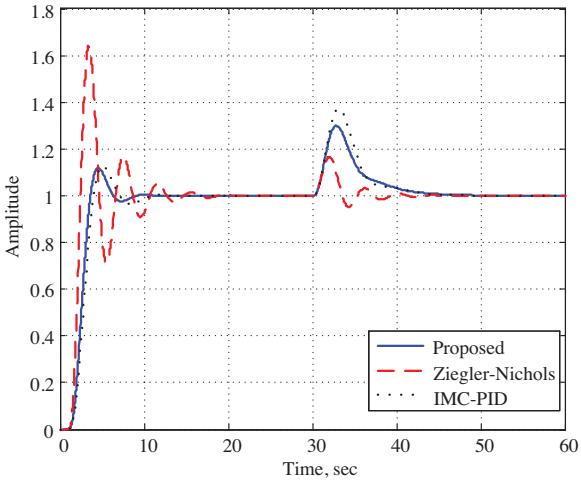

Fig. 11. The time responses comparison of the control systems in example 2 that were tuned by the proposed method and conventional methods.

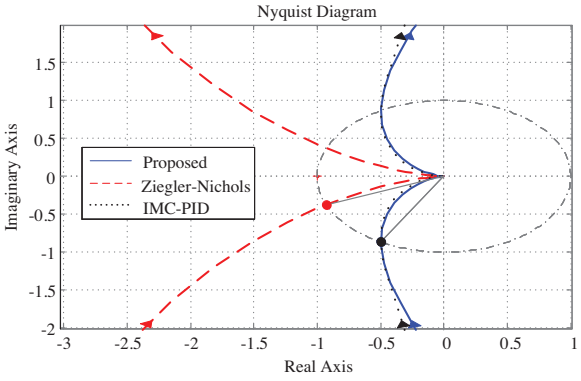

Fig. 12. The Nyquist curves comparison of the control system in example 2 with different PID controller parameters.

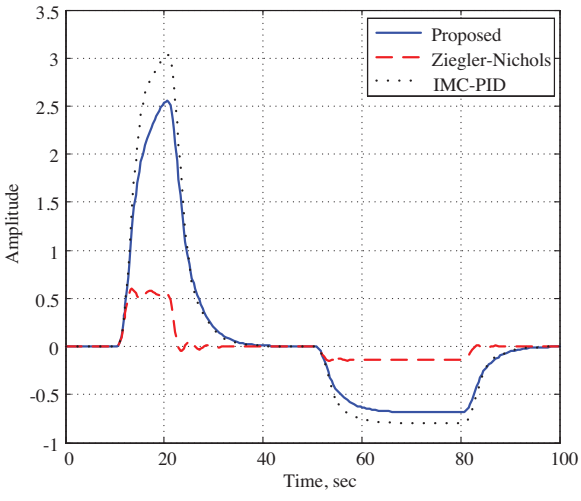

Fig. 13. Influence of the ramp disturbance to the transient responses in example 2.

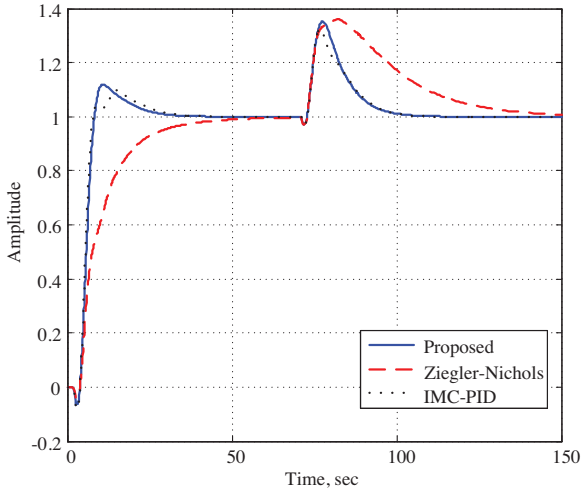

Fig. 14. The time responses comparison of the control systems in example 3 that were tuned by the proposed method and the conventional methods.

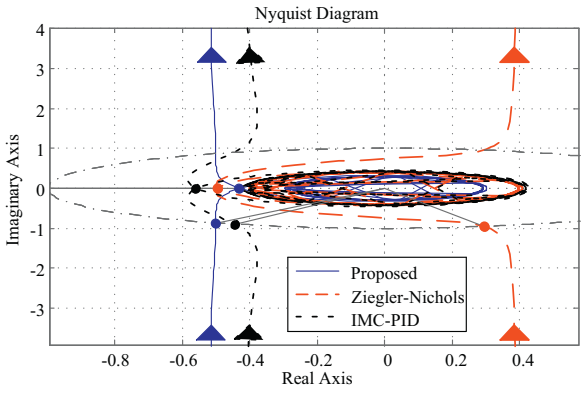

Fig. 15. The Nyquist curves comparison of the control system in example 3 with different PID controller parameters.

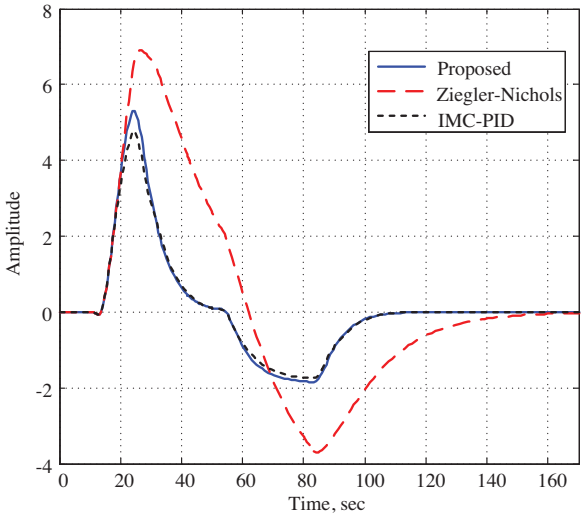

Fig. 16. Influence of the ramp disturbance to the transient responses in example 3.

reported in Fig. 8. In addition, the influence of ramp disturbances on the control system is studied too (Figs. 9 and 10).

Table 2 and Figs. 11–19 present the comparative results of the performance of the proposed method with respect to the IMC-PID [11,12] and the Ziegler–Nichols PID [15]. For the sake of clarity, the same ramp disturbance of Fig. 9 is implemented into the examples 2–4.

The comparison shows that the controller tuned by means of the proposed method is effective and the control system operating with such a controller is characterized by a smaller overshoot, smaller

Table 2
Controller parameters and stability indices of the observed control systems.

Example	Plant model	Method	k_p	k_i	k_d	Phase margin, deg	M_s
2	$\frac{1}{(s+1)^3}$	Proposed method	2.4869	0.7296	1.2353	60	1.4278
		Ziegler–Nichols	5.8118	3.6031	2.3436	21.7962	2.8448
		IMC-PID	1.7942	0.6265	0.6217	60.0159	1.4722
3	$\frac{(-s+1)e^{-5}}{(6s+1)(2s+1)}$	Proposed method	2.1753	0.2696	3.4986	60	1.2693
		Ziegler–Nichols	1.3605	0.0972	4.7619	107.12	1
		IMC-PID	2.4285	0.2857	4.9999	63.5872	1.3347
4	$\frac{e^{-0.1s}}{s^2+1.5s+1}$	Proposed method	1.5033	0.9558	0.5916	70	1.6878
		Ziegler–Nichols	6.7241	7.9257	1.4262	24.71	1.3096
		IMC-PID	1.1381	0.6657	0.2115	69.97	1.6971

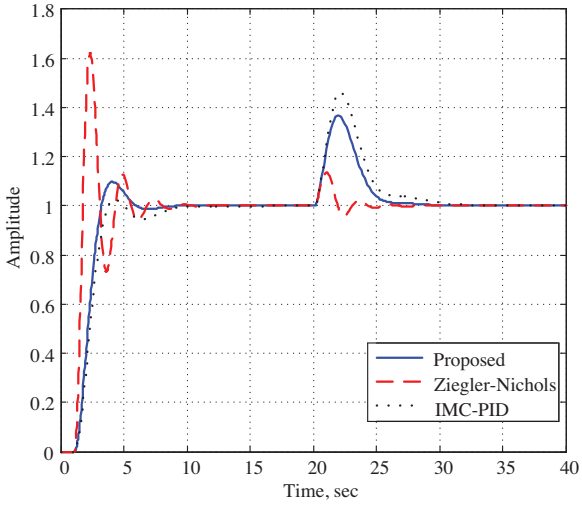

Fig. 17. The time responses comparison of the control systems in example 4 that were tuned by the proposed method and the conventional methods.

setting time, and lower oscillations in the process dynamics with respect to the selected alternatives from the state-of-the-art.

The proposed method allows to tune the PID controller according to the specific control system requirements (such as providing the minimum overshoot, monotone step response, etc.). The method is based on the analytical relations between the robustness and the PID controller parameters. It provides the synthesis of PID controllers for high-order plants. Nevertheless, the user has to set it manually or solve an optimization task to find the crossover frequency. Moreover, according to the examples above, the proposed method might be ineffective in the case of ramp disturbance influence.

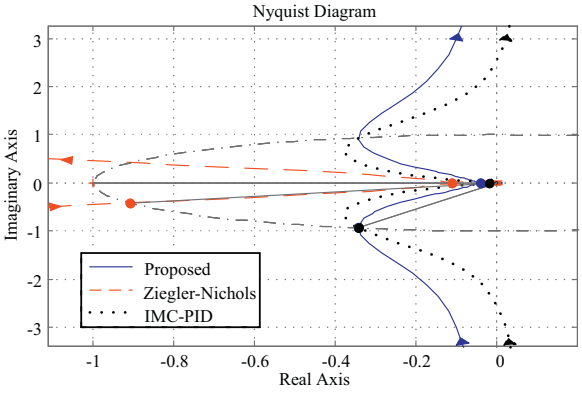

Fig. 18. The Nyquist curves comparison of the control system in example 4 with different PID controller parameters.

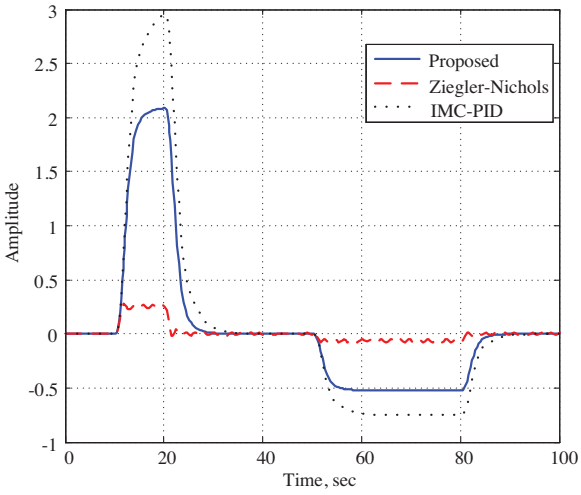

Fig. 19. Influence of the ramp disturbance to the transient responses in example 4.

5. Conclusions

A new method for the PID-controller tuning providing the preset phase margin in the system is proposed. The specific features of this method are the small overshooting and the possibility to provide the required type of the system transfer characteristics by changing the crossover frequency.

The selection of the optimal crossover frequency of the automatic control system is performed based on the integral performance index (ITAE). Actually, the user could find a crossover frequency either manually or via an optimization procedure, providing the IAE, ISE or others. Several tuning methods for PID-regulators are implemented and compared each other showing the benefits of the proposed method and emphasizing its usefulness as an original and novel strategy for PID controllers tuning in single-loop control systems.

Acknowledgements

Authors gratefully acknowledge the Russian Federation government-sponsored Program “Science” at the Tomsk Polytechnic University for the research funding.

References

[1] A. Visioli, Research trends for PID controllers, Acta Polytech. 52 (5) (2012) 144–150.
[2] K.J. Åström, T. Hägglund, The future of PID control, Cont. Eng. Pract. 9 (11) (2001) 1163–1175.
[3] M. Shamsuzzoha, S. Skogestad, The setpoint overshoot method: a simple and fast closed-loop approach for PID tuning, Process Cont. 20 (10) (2010) 1220–1234.

[4] Q.-G. Wang, Z. Zhang, K.J. Astrom, L.S. Chek, Guaranteed dominant pole placement with PID controllers, Process Cont. 19 (2) (2009) 349–352.
[5] D.-J. Wang, Synthesis of PID controllers for high-order plants with time-delay, Process Cont. 19 (2) (2009) 349–352.
[6] S.E. Hamamci, N. Tan, Design of PI controllers for achieving time and frequency domain specifications simultaneously, ISA Trans. 45 (2006) 529–543.
[7] K.J. Åström, T. Hägglund, Advanced PID Control, ISA Press, Research Triangle Park, USA, 2006.
[8] K.J. Åström, R.M. Murray, Feedback Systems: An Introduction for Scientists and Engineers, Princeton University Press, USA, 2008.
[9] E.I. Yurevich, Theory of Automatic Control, Energy, Saint Petersburg, 1975.
[10] K.J. Åström, T. Hägglund, PID Controllers: Theory, Design and Tuning, Instrument Society of America, USA, 1995.
[11] D.E. Rivera, M. Morari, S. Skogestad, Internal model control. 4. PID controller design, Ind. Eng. Chem. Process Des. Dev. 25 (1986) 252–265.
[12] Ahmad Ali, Somanath Majhi, PI/PID controller design based on IMC and percentage overshoot specification to controller setpoint change, ISA Trans. 48 (1) (2009) 10–15.
[13] L.M. Waghmare, G.M. Malwatkar, Design of PID controllers for improved performance of higher order systems, in: UKACC International Conference on Control-2010, UK: Coventry, vol. 4, 2010, pp. 1160–1165.
[14] Q. Wang, T. Lee, H. Fung, Q. Bi, Y. Zhang, PID tuning for improved performance, IEEE Trans. Cont. Syst. Technol. 7 (4) (1999) 457–465.
[15] J.G. Ziegler, N.B. Nichols, Optimum settings for automatic controllers, Trans. A.S.M.E. 64 (1942) 759–768.